



Fast amplitude-modulated pulse trains with frequency sweep (SW-FAM) in solid-state NMR of spin-7/2 nuclei

Thomas Bräuniger^{a,*}, P.K. Madhu^b

^a Institute of Physics, University of Halle, Friedemann-Bach-Platz 6, DE-06108 Halle, Germany

^b Department of Chemical Sciences, Tata Institute of Fundamental Research, Homi Bhabha Road, Colaba, Mumbai 400005, India

ARTICLE INFO

Article history:

Received 11 March 2008

Revised 14 April 2008

Available online 20 April 2008

Keywords:

Quadrupolar nuclei

Sensitivity enhancement

SW-FAM

7QMAS

ABSTRACT

We here investigate the sensitivity enhancement of central-transition NMR spectra of quadrupolar nuclei with spin-7/2 in the solid state, generated by fast amplitude-modulated RF pulse trains with constant (FAM-I) and incremented pulse durations (SW-FAM). Considerable intensity is gained for the central-transition resonance of single-quantum spectra by means of spin population transfer from the satellite transitions, both under static and magic-angle-spinning (MAS) conditions. It is also shown that incorporation of a SW-FAM train into the excitation part of a 7QMAS sequence improves the efficiency of 7Q coherence generation, resulting in improved signal-to-noise ratio. The application of FAM-type pulse trains may thus facilitate faster spectra acquisition of spin-7/2 systems.

© 2008 Elsevier Inc. All rights reserved.

1. Introduction

Most atomic nuclei observable by nuclear magnetic resonance (NMR) spectroscopy have half-integer spin $I > 1/2$, and thus possess a quadrupolar moment [1–3]. Recently, a number of solid-state NMR studies has been published involving nuclei with spin $I = 7/2$, such as ^{43}Ca [4–6], ^{45}Sc [7–9], ^{49}Ti [10–12], ^{51}V [13–15], ^{139}La [16,17], or a combination of these isotopes [18]. The purpose of such studies is to determine the chemical shift and the quadrupolar interaction parameters, and to correlate them to structure and properties of the compounds under investigation. In most cases, the solid-state NMR characterisation of materials containing quadrupolar nuclei is restricted to observing the position and shape of the second-order quadrupolar broadened central-transition peak, either under static or magic-angle spinning (MAS) conditions. If the characteristic ‘second-order shape’ of the central-transition peak can be observed, the NMR interaction parameters may be determined from one-dimensional spectra [1–3]. A more precise determination is possible by using two-dimensional methods such as MQMAS spectroscopy [19–21], which add a high-resolution dimension.

The acquisition of NMR spectra of spin-7/2 systems is often hampered by inherently low sensitivity, due to small gyromagnetic ratios, low natural abundance, strong quadrupolar interaction or by any combination of these factors (see Table 1). For one-dimensional spectra, the intensity of the central-transition (CT) signal can be increased by transferring spin population from the satellite

transitions (ST). Complete inversion of the ST’s of a spin I leads to an enhancement of the CT intensity by a factor of $2I$, while complete saturation of the ST’s (see Fig. 1a) results in an improvement factor of $I + 1/2$. The apparently first experimental evidence showing enhancement of the CT as a result of manipulation of the ST’s was published by R.V. Pound already in 1950 [24]. Since the re-introduction of this principle by Vega and Naor in 1981 [25], and by Haase et al. [26–28] in a series of detailed papers, several experimental techniques have been put forward to effect the necessary manipulations of the ST’s [29–44]. Among these techniques are double frequency sweeps (DFS) [29–33], the application of hyperbolic secant pulses (HS) [45] to quadrupolar nuclei [34–36], and the use of pulse trains with alternating phases, designated either ‘rotor assisted population transfer’ (RAPT/FSG-RAPT) [37–39] or ‘fast amplitude-modulated’ (FAM) pulse trains [40–44]. (More details about these methods and their development may be found in the introductions of Refs. [36] and [44].)

The problem of low sensitivity is especially severe for acquisition of MQMAS spectra, because of the low efficiency of excitation and conversion of multiple-quantum coherences. The most widespread application of MQMAS is in the form of the three-quantum (3Q) experiment [21], which can be performed on all nuclei with half-integer spin $I \geq 3/2$, and may be acquired with a reasonable signal-to-noise ratio. However, the sensitivity problem becomes progressively worse when attempting to observe higher coherence orders (five-, seven-, and nine-quantum) for nuclei with spin quantum numbers larger than 3/2. For spin-7/2 nuclei, the ratio of the respective 3Q:5Q:7Q signals has been estimated to be $6\frac{2}{3} : 2\frac{2}{3} : 1$ [41]. Nevertheless the acquisition of 5Q, 7Q or 9Q spectra is of interest, as for some samples they may yield a substantial

* Corresponding author. Fax: +49 345 5527161.

E-mail address: thomas.braeuniger@physik.uni-halle.de (T. Bräuniger).

Table 1
Properties of quadrupolar nuclei with spin-7/2

Nuclide	Spin I	Q values ^a (mb)	Natural abundance (%) ^b	ν_0 at $B_0 = 9.40$ T ^c (MHz)	Relative receptivity ^d
⁴³ Ca	7/2	−40.8	0.135	26.975	2.87×10^{-5}
⁴⁵ Sc	7/2	−220	100.0	97.375	1.00
⁴⁹ Ti	7/2	247	5.41	22.605	6.77×10^{-4}
⁵¹ V	7/2	−52	99.75	105.405	1.26
⁵⁹ Co	7/2	420	100	94.730	9.21×10^{-1}
¹²³ Sb	7/2	−490	42.79	52.200	6.59×10^{-2}
¹³⁹ La	7/2	200	99.91	56.975	2.00×10^{-1}
¹³³ Cs	7/2	−3.43	100	52.859	1.60×10^{-1}
¹⁷⁷ Hf	7/2	3365	18.60	16.247	8.64×10^{-4}
¹⁸¹ Ta	7/2	3170	99.99	48.529	1.24×10^{-1}

^a Q values of quadrupole moment eQ in millibarn ($1 \text{ mb} = 10^{-31} \text{ m}^2$), from Ref. [22].

^b From Ref. [23].

^c Calculated using the gyromagnetic ratios γ listed in Ref. [23].

^d Relative receptivity normalised to ⁴⁵Sc. The absolute receptivity A is defined [23] as $A = \gamma^3 x I(I+1)$, where x is the natural abundance, and γ the gyromagnetic ratio of the nucleus, $\gamma = (2\pi\nu_0)/B_0$. Thus, the absolute receptivity used as a reference is $A(^{45}\text{Sc}) = 4.3429 \times 10^{24} \text{ rad}^3 \text{ s}^{-3} \text{ T}^{-3}$, which is about one third of the receptivity of protons, $A(^1\text{H}) = 1.4358 \times 10^{25} \text{ rad}^3 \text{ s}^{-3} \text{ T}^{-3}$.

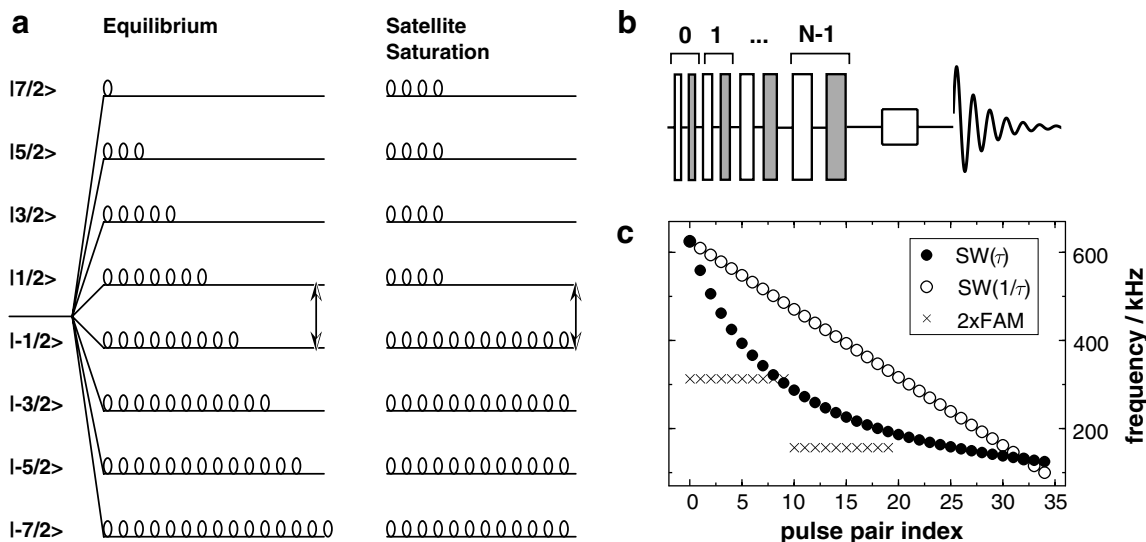


Fig. 1. (a) Schematic representation of spin population distribution for an $I = 7/2$ nucleus in an external magnetic field. The spectral intensity for the central-transition ($m = -1/2 \rightarrow +1/2$) is proportional to the population difference. In the case of full saturation of the satellite transitions, the achieved enhancement factor for the central-transition signal is $(I + 1/2)$, while for complete inversion of the satellite transitions (not shown), the enhancement factor is $2I$. (b) Schematic representation of the RF pulse progression in an SW-FAM pulse train sweeping from higher to lower modulation frequencies followed by a read pulse and the resulting FID. Above the SW-FAM train, the pulse pair index is indicated, while the alternating white and grey colours of the pulses signify the 180° phase shift. (c) Modulation frequencies generated by FAM pulse trains, with the parameters used for acquiring the ⁴⁵Sc NMR spectra shown in Fig. 2. Open circles show the SW($1/\tau$)-FAM train; filled circles depict the SW(τ)-FAM train; crosses represent the double-block FAM-I with two modulation frequencies.

improvement in resolution [46]. Because of the poor signal-to-noise ratio of MQMAS spectroscopy, numerous efforts have been devoted to achieving better sensitivity [20,21].

In this paper, we focus on sensitivity enhancement of both MAS and 7QMAS spectra of spin-7/2 nuclei by using fast amplitude-modulated (FAM) pulse trains, in particular the use of FAM pulse trains with swept modulation frequency (SW-FAM) [42–44]. It is demonstrated that application of SW-FAM sequences results in considerable improvement of the signal-to-noise ratio, which directly translates into time saving when acquisition of NMR spectra of spin-7/2 nuclei is required, as in the studies in Refs. [4–18].

2. Sensitivity enhancement of single-quantum spectra

The idea underlying the fast amplitude-modulation (FAM) approach is to generate sidebands of the RF carrier (=Larmor) frequency ω_0 using a series of pulse pairs, with each of the pairs consisting of two RF pulses with a 180° phase shift between them. The simplest FAM pulse train (“FAM-I”) is formed by a

block of pulse pairs of uniform duration τ_p , separated by constant interpulse delays, which are usually of duration τ_p as well. Such uniform pulse pairs produce strong main sidebands at $\omega_0 + \omega$ and $\omega_0 - \omega$, with ω determined by the pulse durations, $\omega = 2\pi/(4\tau_p)$, plus higher-order sidebands (the next being at $\omega_0 \pm 3\omega$), which are however much weaker. This can be demonstrated by Fourier transformation of the time-domain representation of a FAM train [44]. By adjusting the pulse durations of the FAM train, an appropriate modulation frequency ω can be chosen to manipulate a satellite transition. However, even for a single crystal spectrum, $(I - 1/2)$ modulation frequencies are needed to traverse all satellite transitions of a nucleus with half-integer spin I . For the usually encountered case of powder samples, the RF effects on the spins additionally vary with the respective orientation of the crystallites. When acquiring spectra under magic-angle spinning conditions, FAM-I pulse trains benefit from the fact that the rotor motion adds another modulation frequency, thus spreading out the effect of the “monochromatic” RF. Therefore, considerable enhancement of central-transition

MAS spectra can be produced by preceding a read pulse by a FAM-I train [6,37,38,40–42].

However, when acquisition of static spectra is required, and/or when the nucleus to be observed has more than one satellite transition (as with spin-7/2), it is desirable to replace the single modulation frequency of FAM-I by a frequency sweep. Such a range of sideband frequencies can be generated by a frequency-swept FAM train (“SW-FAM”), where the durations of the RF pulse pairs are changed continuously within the pulse train, as shown schematically in Fig. 1b. The sweep of modulation frequency may be carried out in different ways. In the original SW-FAM scheme [42], constant time increments Δ are added to the duration of both the RF pulses and interpulse delays τ_p . Thus, a pulse train starting with a modulation period of $\tau^0 = 4\tau_p^0$ for the first FAM pulse pair, would finish with a modulation period $\tau^{N-1} = 4\tau_p^{N-1}$ after the execution of N pulse pairs, with $\tau_p^{N-1} = \tau_p^0 + (N-1)\Delta$. This produces a curved distribution of frequencies, as shown in Fig. 1c (filled circles). Because the modulation periods τ^i for the i th pulse pair are being incremented linearly, such pulse trains are designated SW(τ)-FAM. An alternative approach is to generate a frequency distribution ($1/\tau^i$) which is linear with respect to the pulse pair progression. The resulting pulse train (see Fig. 1c, open circles) is referred to as SW($1/\tau$)-FAM, and gives better enhancement for static samples compared to SW(τ)-FAM because of the even distribution of modulation frequencies [44]. The necessary formulae to compute the pulse trains for both SW(τ)- and SW($1/\tau$)-FAM may be found in Ref. [44].

Four parameters define a SW-FAM train, namely the duration of the first and last pulses, τ_p^0 and τ_p^{N-1} (which limit the sweep window), the number N of pulse pairs employed, and the RF strength. For the application of FAM-I trains to spin-7/2 nuclei, the single crystal case suggests the use of three FAM-I blocks with different modulation frequencies, to manipulate the $(I-1/2)=3$ satellite transitions. To keep the number of adjustable parameters within the same range of the SW-FAM trains, only two FAM-I blocks are used, with the parameters $N_a = N_b$, τ_p^a , and τ_p^b . This is the same approach as used in Ref. [41] for signal-enhancement of spin-7/2 spectra using FAM-I sequences for polycrystalline samples. The performance of the respective (SW-)FAM pulse trains applied for signal-enhancement needs to be optimised for a given sample by adjusting the relevant parameters. For the results presented here, the pulse train parameters were optimised for static samples, and subsequently also used for enhancement of MAS spectra. The actual values of the parameters may be found in the respective figure captions.

We first address the enhancement of the CT line intensity of spin-7/2 spectra using FAM and SW-FAM pulse trains for single-quantum spectra, both under static and MAS conditions. As a sample compound, scandium sulphate ($\text{Sc}_2(\text{SO}_4)_3$) was used, since $^{45}\text{Sc}(I=7/2)$ possesses comparatively good sensitivity, as can be seen from Table 1. The quadrupolar coupling constant χ and the asymmetry parameter η of the three ^{45}Sc sites existing in this sample are ($\chi_1 = 5.2$ MHz, $\eta_1 = 0.1$), ($\chi_2 = 4.3$ MHz, $\eta_2 = 0.8$), and ($\chi_3 = 4.5$ MHz, $\eta_3 = 0.5$) [46]. The ^{45}Sc spectra were acquired on a VARIAN INOVA 400 spectrometer, with a Larmor frequency of $\nu_0(^{45}\text{Sc}) = 97.108$ MHz, using a CHEMAGNETICS 4 mm MAS probe. For spectra acquisition, a Hahn-echo sequence with a 16-step phase cycle and an echo period of one rotor period was used, with 48 and 80 transients accumulated for MAS and static spectra, respectively. The Hahn echo was preceded by FAM or SW-FAM trains for spin population transfer, with the central-transition RF nutation frequencies being $\nu_{\text{nut}}(\text{FAM}) \approx 75$ kHz, and $\nu_{\text{nut}}(\text{echo}) \approx 25$ kHz. To avoid detection of unwanted coherences, the pulses of the FAM trains were phase-cycled in conformity with the phase of the $\pi/2$ pulse of the echo sequence (i.e. $0^\circ + \Phi_{\pi/2}$ and $180^\circ + \Phi_{\pi/2}$).

To further substantiate the signal-enhancement performance of FAM and SW-FAM sequences, numerical simulations were carried out using the SIMPSON package [47]. For these calculations, the quadrupolar parameters of only one of the existing three ^{45}Sc sites were used, i.e. $\chi_3 = 4.5$ MHz and $\eta_3 = 0.5$, as they constitute an approximate average of the three sites. The static ^{45}Sc central-transition signal was calculated considering 28,656 powder orientations according to the ZCW scheme [47], whereas 4180 ZCW orientations plus 10 γ -angles for each orientation were used for calculation of the MAS spectra. To obtain enhancement factors, the total signal intensity of the spectrum with preceding (SW-)FAM train and read pulse was compared to the corresponding single-pulse spectrum, by summing up the intensities of all calculated spectral points.

Examples of enhanced ^{45}Sc NMR central-transition spectra of scandium sulphate at 10 kHz MAS, in comparison to the non-enhanced spectra, are depicted in Fig. 2. At this spinning speed, the best enhancement is achieved by using the double-block FAM-I or the SW(τ)-FAM train, with SW($1/\tau$)-FAM being slightly less efficient. The evolution of the enhancement factors going from static conditions to 10 kHz MAS is plotted in Fig. 3. As expected, the SW($1/\tau$)-FAM delivers the best enhancement for static samples, but drops in efficiency with the onset of sample rotation. The double-block FAM-I train, in contrast, performs very poorly for the static case, but gives much better enhancement for spinning samples. This may partly be attributed to a population transfer process via adiabatic level crossings induced by the sample rotation (the acronym RAPT [37–39], “rotor assisted population transfer”, refers to this process). The SW(τ)-FAM sequence constitutes a compromise between these two situations, performing fairly well under both static and MAS conditions. In Fig. 1c, it can be seen that the curved frequency distribution of SW(τ)-FAM leads to a “bunching” in the region of lower frequencies, in fact in the same region where the optimal modulation frequency of the second FAM-I block is located. The improved performance of SW(τ)-FAM over SW($1/\tau$)-FAM may thus be due to its similarity to a FAM-I distribution in the last part of the pulse train, although the exact nature of the transfer process needs to be studied in more detail. Numerical simulations of the enhancement factors (Fig. 3b) produce results very similar to those obtained experimentally (Fig. 3a). Since the probe response to RF is of no concern in the simulations, the overall enhancement can be slightly pushed up by increasing the number of pulse pairs to $N=50$ for the SW-FAM trains and $N_a = N_b = 25$ for the double-block FAM-I, which gives factors about 20% higher than those determined by experiment. When carrying out simulations with the number of pulse pairs used in the experiments ($N=35$, $N_a = N_b = 10$), the resulting enhancement factors follow the experiment more closely, overestimating the experimental values by about 5–10%.

A similar picture as described for enhancement of ^{45}Sc spectra was obtained for ^{43}Ca . Numerical simulations were carried out for the quadrupolar parameters of CaTiO_3 , $\chi = 2.13$ MHz and $\eta = 0.7$ [48]. When plotting the enhancement factors over MAS speed (Fig. 4), the observed effect of the respective FAM trains is analogous to that for ^{45}Sc shown in Fig. 3. It proved however impossible to verify these findings by experiment using a CaTiO_3 sample with ^{43}Ca in natural abundance, as a time-consuming attempt convinced us, and an isotopically labelled sample was unfortunately not at our disposal. Given the nearly identical behaviour of experiment and simulation for ^{45}Sc spectra, it may be expected that the plot in Fig. 4 closely approximates the experimental situation. In fact, use of only one FAM-I block may be sufficient to already deliver significant enhancement of the ^{43}Ca signal under MAS, as exemplified by a recent study of hydroxyapatites by Smith and co-workers [6].

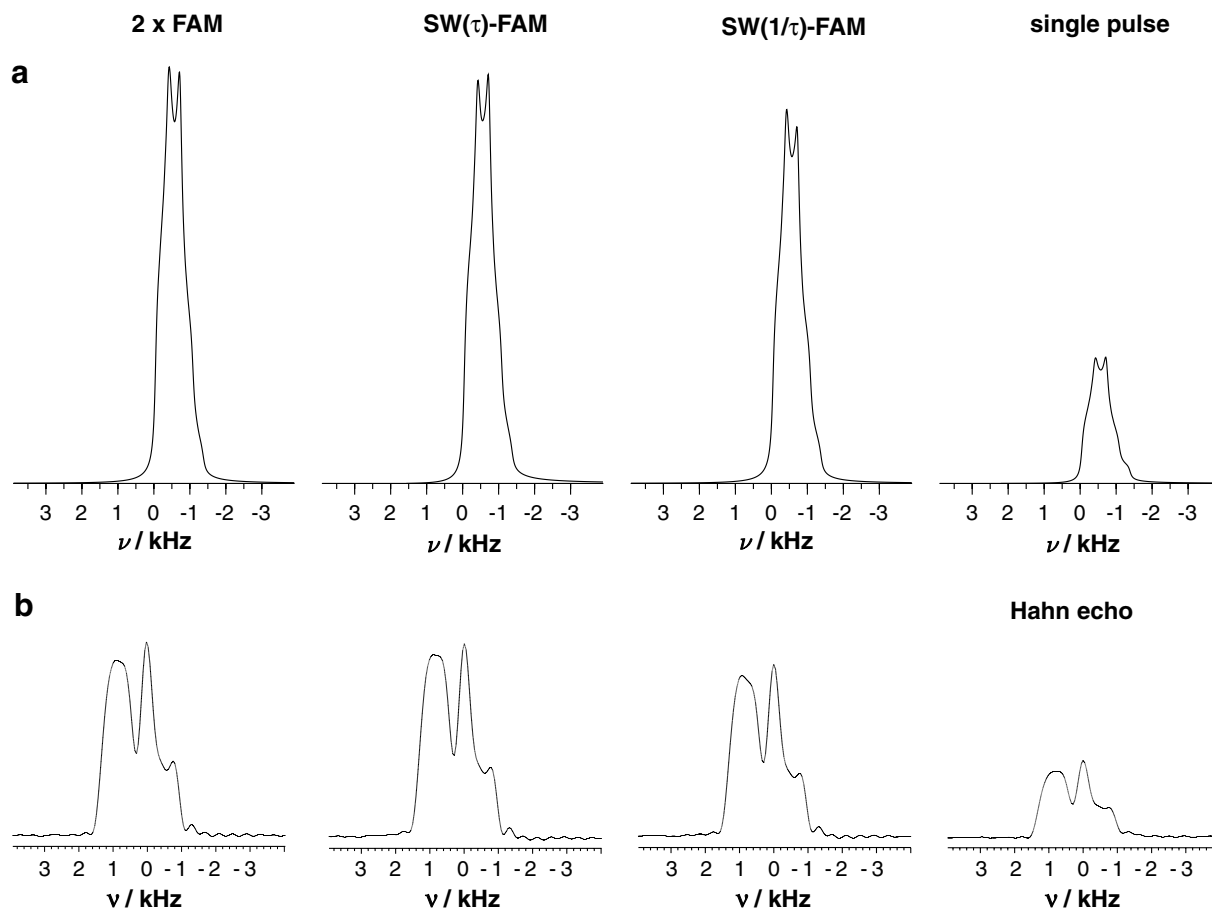


Fig. 2. ^{45}Sc NMR spectra of the central-transition line at 10 kHz MAS, obtained by preceding the read sequence with FAM or SW-FAM pulse trains. (a) Simulated spectra were calculated with the SIMPSON package [47], using quadrupolar parameters $\chi = 4.5$ MHz and $\eta = 0.5$ as an approximate average of the three ^{45}Sc sites existing in $\text{Sc}_2(\text{SO}_4)_3$ [46], and therefore have a different appearance from the experimental spectra. The parameters of the SW($1/\tau$)-FAM train were $N = 50$, $\tau_p^0 = 0.4$ μs to $\tau_p^{49} = 2.5$ μs ; of the SW(τ)-FAM train $N = 50$, $\tau_p^0 = 0.4$ μs to $\tau_p^{49} = 2.0$ μs , and of the double-block FAM-I with two modulation frequencies $N_a = N_b = 25$, $\tau_p^a = 0.8$ μs , and $\tau_p^b = 1.6$ μs . (b) Experimental spectra were recorded for scandium sulphate, $\text{Sc}_2(\text{SO}_4)_3$, using a recycle delay of 10 s (to avoid saturation effects), and an acquisition time of 2.5 ms. The pulse durations of the FAM trains were identical to those listed in (a), but a smaller number of pulse pairs was employed: $N = 35$, and $N_a = N_b = 10$. Further details on the NMR experiments and numerical simulation are given in the text.

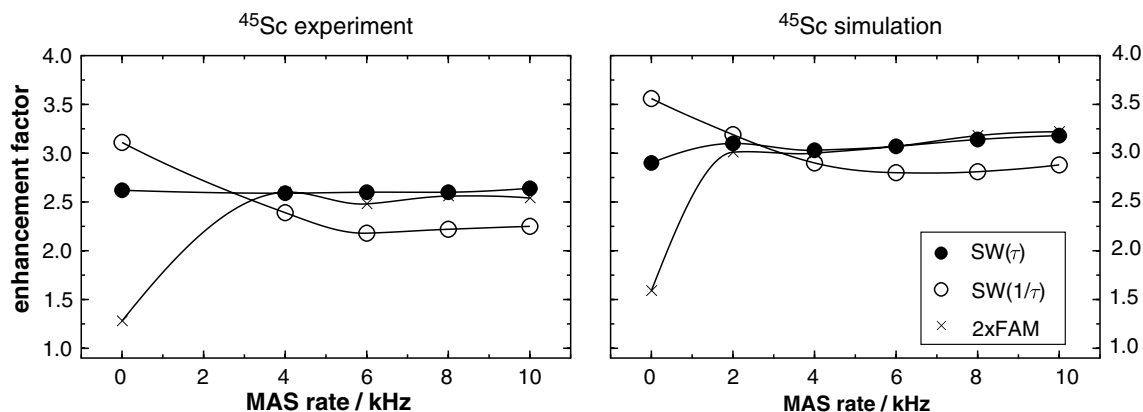


Fig. 3. Evolution of enhancement factors of ^{45}Sc NMR spectra with increasing MAS speed. Experimental spectra were acquired for scandium sulphate, $\text{Sc}_2(\text{SO}_4)_3$. The simulated spectra were calculated with the SIMPSON package [47]. The same parameters as given in the caption of Fig. 2 were used for experiments and simulations. Open circles show the SW($1/\tau$)-FAM train, filled circles depict the SW(τ)-FAM train, and crosses represent the double-block FAM-I with two modulation frequencies. The fitted lines are drawn to guide the eye.

We also explored the dependence of the signal-enhancement on the magnitude of the quadrupolar coupling constant χ for ^{45}Sc , as shown in Fig. 5. To this end, we optimised the performance the SW-FAM trains for the mid-point of the graph, i.e. for the quadru-

polar parameters $\chi = 4.5$ MHz and $\eta = 0.0$. The best signal enhancement was found for pulse trains with parameters differing only slightly from those giving the best performance for the combination $\chi = 4.5$ MHz and $\eta = 0.5$, for which the enhancement factors

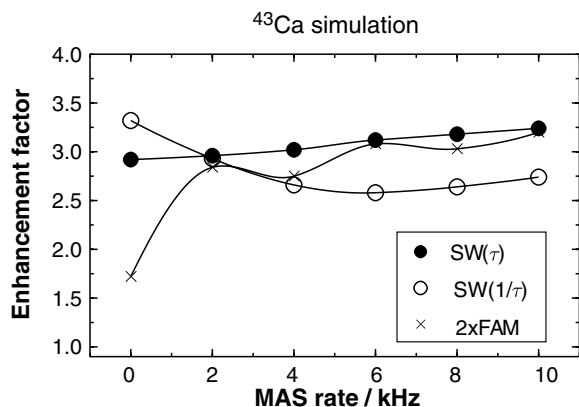


Fig. 4. Evolution of enhancement factors of ^{43}Ca central-transition spectra with MAS speed. Spectra were calculated for the quadrupolar parameters of CaTiO_3 , $\chi = 2.13$ MHz and $\eta = 0.7$ [48] with the SIMPSON package [47]. The parameters of the SW(1/τ)-FAM train (open circles) were $N = 50$, $\tau_p^0 = 0.4$ μs to $\tau_p^{49} = 4.0$ μs; of the SW(τ)-FAM train (filled circles) $N = 50$, $\tau_p^0 = 0.4$ μs to $\tau_p^{49} = 3.3375$ μs, and of the double-block FAM-I (crosses) with two modulation frequencies $N_a = N_b = 25$, $\tau_p^a = 1.2$ μs, and $\tau_p^b = 2.4$ μs. The fitted lines are drawn to guide the eye.

are shown in Fig. 3. This fact already indicates that for small changes in the magnitudes of the quadrupolar parameters χ and η , only small adjustments of the pulse trains are needed to keep best performance. The flatness of the curves in Fig. 5 further demonstrates that a SW-FAM train optimised for one combination of χ and η maintains good enhancement over a broad range of χ . Below $\chi \approx 2.5$ MHz, a steep decline of enhancement is seen, which has been observed in similar fashion for ^{27}Al before [44]. This decrease is due to the fact that the method of spin population transfer relies on the existence of a reasonably sized quadrupolar moment to shift the satellite transitions away from the central transition. Above $\chi \approx 4.0$ MHz, application of SW-FAM trains results in useful signal-enhancement for the ^{45}Sc spectra over a wide range of χ , with SW(1/τ)-FAM performing somewhat better under static, and SW(τ)-FAM under MAS conditions. We estimate that for ^{45}Sc samples, good signal-enhancement may be obtained by using a first pulse duration of $\tau_p^0 = 0.3$ – 0.5 μs, and a last pulse duration of $\tau_p^{N-1} = 2.0$ – 3.0 μs. Depending on the RF load that can be handled by the probe, $N = 30$ – 50 pulse pairs may be used, with the RF strength as high as possible. While the duty cycle of a SW-FAM

train is only 50%, it should be kept in mind that the total duration of the pulse train is in the range of 200–300 μs. The authors usually employ RF nutation frequencies which are about 75% of those used for excitation and conversion pulses in MQMAS. Pulse programs for VARIAN INOVA and a calculation tool for SW-FAM pulse trains are available for download from http://www.physik.uni-halle.de/nmr/dir_tb/swfam.html.

Concerning the magnitude of the enhancement factors discussed here, the theoretical enhancement limit for complete saturation of the satellite transitions, namely $I + 1/2 = 4$, is reached only for the calculated ^{45}Sc spectra shown in Fig. 5, with all other factors being below that. The overall enhancement does however not necessarily allow conclusions about the state of individual ST's in the sample. It has been shown for application of DFS under MAS conditions [33] that the observed enhancement in a powder sample is a result of partial saturation and inversion of the ST's, dispersed among the affected crystallites. In the case of ^{43}Ca and ^{45}Sc , the combined effects of saturation and inversion realised by the application of (SW-)FAM trains result in enhancement factors of around 3.5 for static, and about 3.0 for rotating samples. While this is already a substantial increase over non-enhanced spectra, the potential of the spin populations of the ST's can be further utilised by using multiple sweep and acquisition cycles before letting the system go back to thermal equilibrium. This technique was first suggested by Kwak et al. [39], was later also applied to the DFS method [49], and very recently has been successfully demonstrated for FAM trains as well [50].

3. Sensitivity enhancement of 7QMAS spectra

Aquisition of two-dimensional MQMAS spectra [19–21] is often a desirable option, as the chemical shift and quadrupolar interaction parameters may be determined more precisely. For spin-7/2 nuclei, either the 3Q, 5Q, or 7Q coherence pathway may be chosen for this purpose, with sensitivity sharply declining for the higher coherence orders [41]. However, for amorphous samples, the spectra of the higher coherence orders are expected to deliver better resolution [46]. In a recent ^{43}Ca NMR study of Ca-containing glasses [4], the 7QMAS indeed appeared to give the most detailed results, even though comparison was made difficult by the use of a magnetic field different from that used for the 3Q- and 5QMAS spectra. Aquisition of the ^{43}Ca -7QMAS spectrum, using simple hard RF pulses, took about 3.5 days [4], despite the fact that ^{43}Ca had been isotopically enriched. A substantial part of this measuring

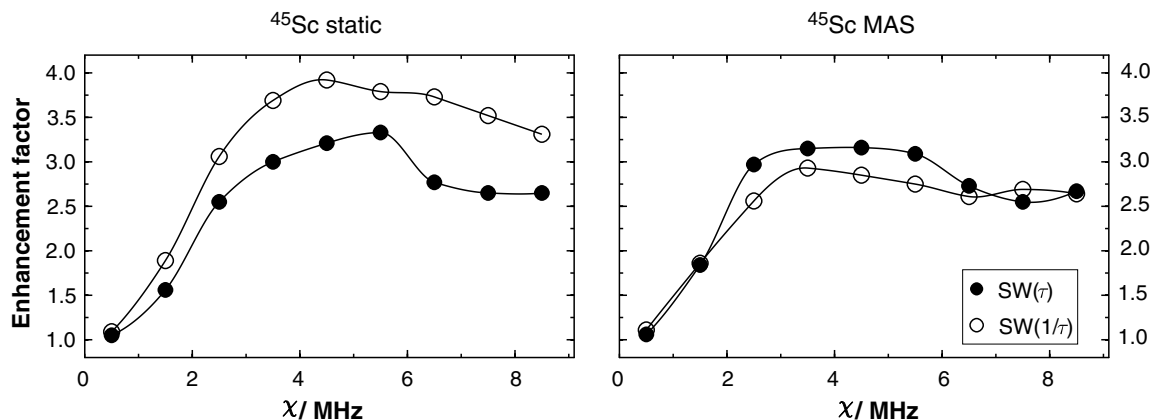


Fig. 5. Evolution of enhancement factors of ^{45}Sc central-transition spectra with magnitude of the quadrupolar coupling constant χ , under both static (left) and 10 kHz MAS conditions (right). The spectra were calculated with the SIMPSON package [47]. The parameters of the SW-FAM trains were optimised for the quadrupolar parameters of $\chi = 4.5$ MHz and $\eta = 0.0$ (mid-point of the graph), and then used for all other χ values. The pulse trains used in the calculations were: SW(1/τ)-FAM train (open circles), with $N = 50$, $\tau_p^0 = 0.35$ μs to $\tau_p^{49} = 2.75$ μs; and SW(τ)-FAM train (filled circles), with $N = 50$, $\tau_p^0 = 0.35$ μs to $\tau_p^{49} = 2.25$ μs. The fitted lines are drawn to guide the eye.

time may be saved by the utilisation of enhancement schemes in both excitation and conversion block of the 7QMAS pulse sequences.

The majority of enhancement schemes developed so far has been aimed at improving the efficiency of the MQ→1Q conversion process. Instead of employing a hard radio-frequency (RF) pulse P_H^{con} , a number of schemes replacing P_H^{con} has been suggested for more efficient conversion, the principles and applications of which have been discussed in recent review articles [20,21]. These pulse schemes include double frequency sweeps (DFS) [30,31], rotationally induced adiabatic coherence transfer (RIACT) [51], hyperbolic secant pulses (HS) [52] and fast amplitude-modulation (FAM) [25,53,54]. Also, soft-pulse added mixing (SPAM) may be used for improved coherence conversion [55,56]. For SPAM, no additional parameters (as compared to a z-filter MQMAS spectrum) need to be optimised [56], which makes it easier to implement than the methods listed above. However, in a recent comparison of FAM and SPAM [57], it was found that FAM may give better maximum enhancement, even though additional parameters need to be adjusted. The utilisation of enhancement techniques for improving excitation efficiency has received less attention. It has been shown that for spin-3/2 nuclei, higher 3Q intensity can be obtained by preceding the RIACT [51] or RIACT-FAM sequence [58] by a FAM block lasting for a rotor period [59–61]. It was also demonstrated that population transfer induced by multiple frequency sweeps (MFS) can improve the initial generation of 3Q coherence for spins with $l = 5/2$ [32]. In 2002, Goldbourt and Vega [62] suggested an improved excitation scheme for creating 5Q coherences of spin-5/2 nuclei, employing a hard RF pulse immediately followed by a FAM-I train. The idea underlying this approach is to convert three quantum coherence (3QC) generated by the initial P_H^{exc} pulse into the desired five quantum coherence (5QC) by use of the FAM train, which induces a population transfer between the $|\pm 3/2\rangle$ and $|\pm 5/2\rangle$ energy levels. The subsequent 5QC→1QC conversion is then effected [62] by means of a amplitude-modulated RF pulses of the FAM-II type [54], consisting of a number of pulses of varying duration and alternating phase, or by a simple FAM-I train [63].

Similarly, for 7QMAS spectra of spin-7/2, two FAM-I blocks may be appended to the initial P_H^{exc} pulse, to realise the transfer 3QC→5QC→7QC, as has been demonstrated before [41]. The same effect can be achieved by using the swept modulation frequency of a SW-FAM train. Since under MAS conditions, SW(τ)-FAM tends to be more efficient (as discussed above), such a pulse train was incorporated into the excitation part of a 7QMAS pulse sequence. The signal intensity gained from a “classical” experiment of two hard RF pulses, $P_H^{\text{exc}} - P_H^{\text{con}}$, was compared to that of using a FAM-I train for coherence conversion, $P_H^{\text{exc}} - \text{FAM-I}$, and finally to the sequence with extended excitation part, $(P_H^{\text{exc}} - \text{SW}(\tau)\text{-FAM}) - \text{FAM-I}$. The 7Q-filtered signal via the coherence pathway 0QC → -7QC → -1QC was acquired using the 28-step phase cycle listed in Table 2. Here, the receiver phase ϕ_{rec} follows from the master equation:

$$\sum_i \Delta p_i \phi_i + \phi_{\text{rec}} = 0$$

Table 2

The 28-step phase cycle used for acquisition of the 7QMAS spectra shown in Fig. 6

Phase	Value (°)
ϕ_{exc}	$\{0, \frac{1 \times 90}{7}, \frac{2 \times 90}{7}, \dots, \frac{27 \times 90}{7}\}$
ϕ_{con}	$\{0\}_{28}$
ϕ_{rec}	$\{0, 90, 180, 270\}_7$

(Subscripts indicate the number of times the phase cycle in parentheses must be repeated.)

with Δp_i being the coherence order change induced by the i th pulse with phase ϕ_i [64,65]. With the phase of the conversion pulse chosen to be zero, $\phi_{\text{con}} = 0$, the calculation simplifies to $\phi_{\text{rec}} = 7\phi_{\text{exc}}$. For spectra acquisition, a 7QC evolution delay of 2 μs was used, in effect acquiring the first t_1 slice of a 2D experiment, and then transforming it in the (anisotropic) F_2 direction. For short evolution delays as used here, the F_2 spectrum can be phased without difficulty, and be used for intensity comparison. A similar approach was employed in a recent work by Kanellopoulos et al. [66], where the efficiency of different MQC conversion schemes was evaluated. A further benefit of pulse sequences comprised only of excitation and conversion parts is that they deliver stronger signal than sequences with a third pulse, such as z-filter [67,68] or split- t_1 [67,69]. These sequences have however clear advantages for acquisition of pure absorptive line shapes in 2D spectra, and the necessary 7QMAS phase cycles (including cogwheel cycles [70]) may be found in Ref. [21]. To determine the best acquisition parameters for the 7QMAS pulse sequences, a sensible optimisation strategy is to obtain an appreciable 7Q signal first by finding the best RF pulse durations for the $P_H^{\text{exc}} - P_H^{\text{con}}$ sequence. Subsequently, the $P_H^{\text{exc}} - \text{FAM-I}$ pulse program can be used to find the best values for the FAM conversion pulse, and finally the full $(P_H^{\text{exc}} - \text{SW}(\tau)\text{-FAM}) - \text{FAM-I}$ sequence with the additional modulation in the excitation part can be optimised. Upon addition of a train of FAM pulses to the excitation block, the optimal duration of the hard excitation pulse P_H^{exc} is found to be slightly shorter compared to the two-pulse sequence, $P_H^{\text{exc}} - P_H^{\text{con}}$, so a re-optimisation of P_H^{exc} is beneficial. This effect has been observed before for 5QMAS spectra of spin-5/2 [63]. The resulting ^{45}Sc -7QMAS spectra of scandium sulphate are shown in Fig. 6. It can be seen that the efficiency of both excitation and conversion part is greatly enhanced by introduction of FAM trains. The relative intensities obtained for the sequences $P_H^{\text{exc}} - P_H^{\text{con}}$, $P_H^{\text{exc}} - \text{FAM-I}$ and $(P_H^{\text{exc}} - \text{SW}(\tau)\text{-FAM}) - \text{FAM-I}$ are approximately 1:3:5. This is very similar to the enhancement obtained with using two consecutive FAM-I blocks in the excitation part, where a factor of 4.0 was observed for ^{139}La -7QMAS spectra of LaAlO_3 [41]. The SW(τ)-FAM holds the advantage of having one less parameter that needs to be optimised, unless the condition $N_a = N_b$ is enforced for the two FAM-I blocks. Since a window of frequencies is swept with SW(τ)-FAM, the range of parameters delivering appreciable signal-enhancement should be larger and therefore easier to find than for FAM-I.

Conceptually, the sweep direction of a SW(τ)-FAM train incorporated into the excitation part of a 7QMAS pulse sequence needs to be reversed from that used for enhancement of a single quantum spectrum. For enhancement of single-quantum spectra, the $|\pm 7/2\rangle$, $|\pm 5/2\rangle$, and $|\pm 3/2\rangle$ energy levels should be consecutively affected, which implies a sweep from higher to lower modulation frequencies. To realise the transfer 3QC→5QC→7QC for 7QMAS, the direction of sweep should go from lower to higher modulation frequencies. (Or, when using two FAM-I blocks, the first one should have a lower modulation frequency than the second, as it was indeed implemented in Ref. [41].) This is intuitively clear in the case of a single crystal, and with some qualification also for static powder samples. Under MAS conditions, however, we found by both numerical simulation and experiment that the observed effects on both single-quantum and 7Q spectra are practically insensitive to the applied sweep direction. The same effect has been reported by Siegel et al. [36] for application of DFS to spin-5/2 systems. A detailed discussion of this complex subject is however outside the scope of this article and will be presented elsewhere. For all spectra shown here, the “conceptually correct” sweep directions have been used.

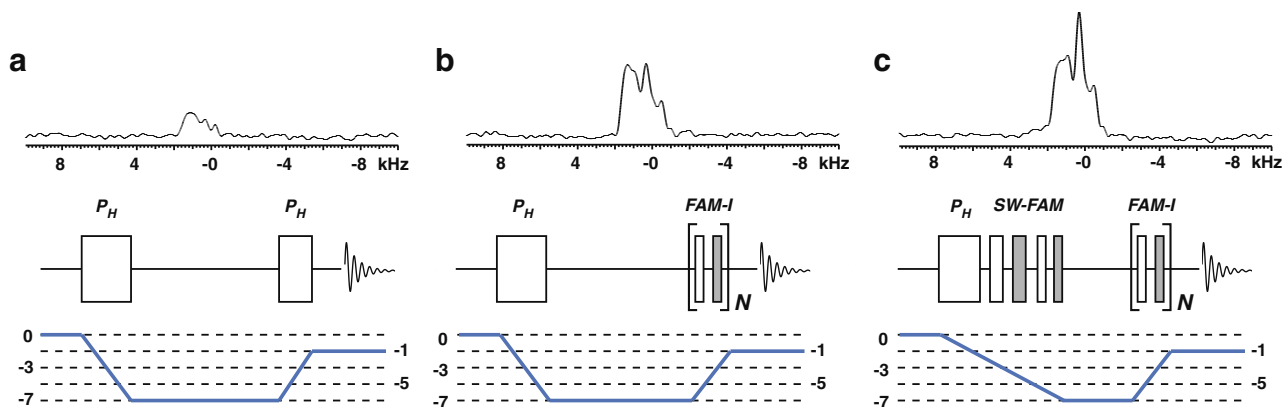


Fig. 6. ^{45}Sc -7QMAS spectra of scandium sulphate, $\text{Sc}_2(\text{SO}_4)_3$ at 8 kHz spinning speed. The spectra were recorded after a 7QC evolution delay of 2 μs , and transformed in the anisotropic F_2 dimension. They were acquired with an RF nutation frequency of $\nu_{\text{nut}} \approx 110$ kHz, using a recycle delay of 5 s, and an acquisition time of 2.5 ms. Two thousand and eight hundred transients were accumulated using the phase cycle listed in Table 2. The coherence pathway is indicated below the spectra. (a) Both excitation and conversion of the 7Q coherence are accomplished by hard RF pulses: $P_{\text{H}}^{\text{exc}} = 6.5$ μs , $P_{\text{H}}^{\text{con}} = 2.5$ μs . (b) Excitation by hard RF pulse, $P_{\text{H}}^{\text{exc}} = 6.5$ μs ; conversion by FAM-I train, with $\tau_{\text{p}} = 1.0$ μs and $N = 6$. (c) Excitation by hard RF pulse, $P_{\text{H}}^{\text{exc}} = 5.5$ μs , followed by a SW(τ)-FAM train with $\tau_{\text{p}}^0 = 1.4$ μs to $\tau_{\text{p}}^{\text{p}} = 0.4$ μs and $N = 10$; conversion by FAM-I train, with $\tau_{\text{p}} = 1.0$ μs and $N = 6$.

4. Conclusions

We have demonstrated how trains of fast amplitude-modulated RF pulses may be usefully employed for enhancing sensitivity when acquiring single-quantum (both under static and MAS conditions) or 7QMAS spectra of quadrupolar nuclei with spin-7/2. For the studied nuclei, ^{43}Ca and ^{45}Sc , the best enhancement of static spectra was obtained using the SW(1/ τ)-FAM sequence [44], whereas for spinning samples, best results were achieved using either double-block FAM-I trains [40,41], or the SW(τ)-FAM sequence [42]. The acquisition of 7QMAS spectra strongly benefits from incorporation of a FAM sequence into the excitation part, similar to what has been reported before for acquisition of 5QMAS spectra of spin-5/2 nuclei [62,63]. Creation of 7Q coherence can be facilitated by either double-block FAM-I [41], or by use of a SW(τ)-FAM sequence, as shown here.

Alternative methods for spin population transfer from the satellite transitions, such as (DFS) [29–33] or hyperbolic secant pulses (HS) [34–36,52] have been shown to give good results for nuclei with spin-3/2 and spin-5/2. They are therefore expected to work well also for spin-7/2 nuclei, although to the best of our knowledge, no application of either DFS or HS to nuclei with $I = 7/2$ has been reported yet. For single-quantum spectra, the best enhancement currently available seems to be the application of multiple sweep and acquisition cycles, as demonstrated in Refs. [39,49,50].

Acknowledgments

Financial support (TB, grant BR 3370/3-1 from Deutsche Forschungsgemeinschaft), and assistance (PKM, from the Department of Science and Technology, India, under SERC FAST Track Scheme) is gratefully acknowledged.

References

- [1] A.J. Vega, Quadrupolar nuclei in solids, in: D.M. Grant, R.K. Harris (Eds.), Encyclopedia of Nuclear Magnetic Resonance, vol. 6, John Wiley & Sons, Chichester, England, 1996, pp. 3869–3889.
- [2] D. Freude, Quadrupolar nuclei in solid state nuclear magnetic resonance, in: R.A. Meyers (Ed.), Encyclopedia of Analytical Chemistry, John Wiley & Sons, Ltd., Tarzana, CA, USA, 2000, pp. 12188–12224.
- [3] A. Jerschow, From nuclear structure to the quadrupolar NMR interaction and high-resolution spectroscopy, Prog. Nucl. Magn. Reson. Spectrosc. 46 (2005) 63–78.
- [4] K. Shimoda, Y. Tobu, Y. Shimoikeda, T. Nemoto, K. Saito, Multiple Ca^{2+} environments in silicate glasses by high-resolution ^{43}Ca MQMAS NMR technique at high and ultra-high (21.8 T) magnetic fields, J. Magn. Reson. 186 (2007) 156–159.
- [5] F. Angeli, M. Gaillard, P. Jollivet, T. Charpentier, Contribution of ^{43}Ca MAS NMR for probing the structural configuration of calcium in glass, Chem. Phys. Lett. 440 (2007) 324–328.
- [6] D. Laurencin, A. Wong, R. Dupree, M. Smith, Natural abundance ^{43}Ca solid-state NMR characterisation of hydroxyapatite: identification of the two calcium sites, Magn. Reson. Chem. 46 (2008) 347–350.
- [7] A.J. Rossini, R.W. Schurko, Experimental and theoretical studies of ^{45}Sc NMR interactions in solids, J. Am. Chem. Soc. 128 (2006) 10391–10402.
- [8] N. Kim, C.-H. Hsieh, J.F. Stebbins, Scandium coordination in solid oxides and stabilized zirconia: ^{45}Sc NMR, Chem. Mater. 18 (2006) 3855–3859.
- [9] C.P. Sebastian, L. Zahng, C. Fehse, R.-D. Hoffmann, H. Eckert, R. Pöttgen, New stannide ScAgSn : determination of the superstructure via two-dimensional ^{45}Sc solid state NMR, Inorg. Chem. 46 (2007) 771–779.
- [10] A. Baldwin, P.A. Thomas, R. Dupree, A multi-nuclear NMR study of the local structure of lead zirconate titanate, $\text{PbZr}_{(1-x)}\text{Ti}_x\text{O}_3$, J. Phys. Condens. Matter. 17 (2005) 7159–7168.
- [11] B. Zalar, A. Lebar, J. Seliger, R. Blinc, V.V. Laguta, M. Itoh, NMR study of disorder in BaTiO_3 and SrTiO_3 , Phys. Rev. B 71 (2005) 64107.
- [12] F.H. Larsen, I. Farman, A.S. Lipton, Separation of ^{47}Ti and ^{49}Ti solid-state NMR lineshapes by static QCPMG experiments at multiple fields, J. Magn. Reson. 178 (2006) 228–236.
- [13] B.A. Gee, Vanadium-51 solid-state NMR electric field gradient tensors: a DFT-embedded ion and isolated cluster study of crystalline vanadium oxides, Solid State Nucl. Magn. Reson. 30 (2006) 171–181.
- [14] N. Poorangsingh-Margolis, R. Renirie, Z. Hasan, R. Wever, A.J. Vega, T. Polenova, ^{51}V solid-state magic angle spinning NMR spectroscopy of vanadium chloroperoxidase, J. Am. Chem. Soc. 128 (2006) 5190–5208.
- [15] W. Huang, A.J. Vega, T. Gullion, T. Polenova, Internuclear ^{31}P - ^{51}V distance measurements in polyoxoanionic solids using rotational echo adiabatic passage double resonance NMR spectroscopy, J. Am. Chem. Soc. 129 (2007) 13027–13034.
- [16] K.J. Ooms, K.W. Feindel, M.J. Willans, R.E. Wasylshen, J.V. Hanna, K.J. Pike, M.E. Smith, Multiple-magnetic field ^{139}La NMR and density functional theory investigation of the solid lanthanum(III) halides, Solid State Nucl. Magn. Reson. 28 (2005) 125–134.
- [17] H. Hamaed, A.Y.H. Lo, D.S. Lee, W.J. Evans, R.W. Schurko, Solid state ^{139}La and ^{15}N NMR spectroscopy of lanthanum-containing metallocenes, J. Am. Chem. Soc. 128 (2006) 12638–12639.
- [18] D. Khabibulin, K. Romanenko, M. Zuev, O. Lapina, Solid state NMR characterization of individual compounds and solid solutions formed in Sc_2O_3 - V_2O_5 - NbO_5 - Ta_2O_5 system, Magn. Reson. Chem. 45 (2007) 962–970.
- [19] L. Frydman, J.S. Harwood, Isotropic spectra of half-integer quadrupolar spins from bidimensional magic-angle spinning NMR, J. Am. Chem. Soc. 117 (1995) 5367–5368.
- [20] L. Frydman, Fundamentals of multiple quantum magic angle spinning NMR on half-integer quadrupolar nuclei, in: D.M. Grant, R.K. Harris (Eds.), Encyclopedia of Nuclear Magnetic Resonance, vol. 9, John Wiley & Sons, Chichester, England, 2002, pp. 262–274.
- [21] A. Goldbourt, P.K. Madhu, Multiple-quantum magic-angle spinning: high-resolution solid-state NMR spectroscopy of half-integer quadrupolar nuclei, Ann. Rep. NMR Spec. 54 (2004) 81–153.
- [22] P. Pyykkö, Spectroscopic nuclear quadrupole moments, Mol. Phys. 99 (2001) 1617–1629.
- [23] R.K. Harris, E.D. Becker, S.M. Cabral de Menezes, R. Goodfellow, P. Granger, NMR nomenclature: Nuclear spin properties and conventions for chemical shifts (IUPAC recommendations 2001), Conc. Magn. Reson. 14 (2002) 326–346.
- [24] R.V. Pound, Nuclear electric quadrupole interactions in crystals, Phys. Rev. 79 (1950) 685–702.

- [25] S. Vega, Y. Naor, Triple quantum NMR on spin systems with $I = 3/2$ in solids, *J. Chem. Phys.* 75 (1981) 75–86.
- [26] J. Haase, M.S. Conradi, Sensitivity enhancement for NMR of the central transition of quadrupolar nuclei, *Chem. Phys. Lett.* 209 (1993) 287–291.
- [27] J. Haase, M.S. Conradi, C.P. Grey, A.J. Vega, Population transfers for NMR of quadrupolar spins in solids, *J. Magn. Reson. A* 109 (1994) 90–97.
- [28] J. Haase, M.S. Conradi, E. Oldfield, Single- and double-resonance experiments of quadrupolar nuclei in solids using sensitivity enhancement of the central transition, *J. Magn. Reson. A* 109 (1994) 210–215.
- [29] E. van Veenendal, B.H. Meier, A.P.M. Kentgens, Frequency stepped adiabatic passage excitation of half-integer quadrupolar spin systems, *Mol. Phys.* 93 (1998) 195–213.
- [30] A.P.M. Kentgens, R. Verhagen, Advantages of double frequency sweeps in static, MAS and MQMAS NMR of spin $I = 3/2$ nuclei, *Chem. Phys. Lett.* 300 (1999) 435–443.
- [31] D. Iuga, H. Schäfer, R. Verhagen, A.P.M. Kentgens, Population and coherence transfer induced by double frequency sweeps in half-integer quadrupolar spin systems, *J. Magn. Reson.* 147 (2000) 192–209.
- [32] D. Iuga, A.P.M. Kentgens, Triple-quantum excitation enhancement in MQMAS experiments on spin $I = 5/2$ systems, *Chem. Phys. Lett.* 343 (2001) 556–562.
- [33] D. Iuga, A.P.M. Kentgens, Influencing the satellite transitions of half-integer quadrupolar nuclei for the enhancement of magic angle spinning spectra, *J. Magn. Reson.* 158 (2002) 65–72.
- [34] R. Siegel, T.T. Nakashima, R.E. Wasylshen, Signal enhancement of NMR spectra of half-integer quadrupolar nuclei in solids using hyperbolic secant pulses, *Chem. Phys. Lett.* 388 (2004) 441–445.
- [35] R. Siegel, T.T. Nakashima, R.E. Wasylshen, Sensitivity enhancement of solid-state NMR spectra of half-integer spin quadrupolar nuclei using hyperbolic secant pulses: Applications to spin-5/2 nuclei, *Chem. Phys. Lett.* 421 (2006) 529–533.
- [36] R. Siegel, T.T. Nakashima, R.E. Wasylshen, Sensitivity enhancement of NMR spectra of half-integer spin quadrupolar nuclei in solids using hyperbolic secant pulses, *J. Magn. Reson.* 184 (2007) 85–100.
- [37] Z. Yao, H.-T. Kwak, D. Sakellariou, L. Emsley, P.J. Grandinetti, Sensitivity enhancement of the central transition NMR signal of quadrupolar nuclei under magic-angle spinning, *Chem. Phys. Lett.* 327 (2000) 85–90.
- [38] S. Prasad, H.-T. Kwak, T. Clark, P.J. Grandinetti, A simple technique for determining nuclear quadrupole coupling constants with RAPT solid-state NMR spectroscopy, *J. Am. Chem. Soc.* 124 (2002) 4964–4965.
- [39] H.-T. Kwak, S. Prasad, T. Clark, P.J. Grandinetti, Enhancing sensitivity of quadrupolar nuclei in solid-state NMR with multiple rotor assisted population transfers, *Solid State Nucl. Magn. Reson.* 24 (2003) 71–77.
- [40] P.K. Madhu, K.J. Pike, R. Dupree, M.H. Levitt, M.E. Smith, Modulation-aided signal enhancement in the magic angle spinning NMR of spin-5/2 nuclei, *Chem. Phys. Lett.* 367 (2003) 150–156.
- [41] P.K. Madhu, O.G. Johannessen, K.J. Pike, R. Dupree, M.E. Smith, M.H. Levitt, Application of amplitude-modulated radiofrequency fields to the magic-angle spinning NMR of spin-7/2 nuclei, *J. Magn. Reson.* 163 (2003) 310–317.
- [42] T. Bräuniger, K. Ramaswamy, P.K. Madhu, Enhancement of the central-transition signal in static and magic-angle-spinning NMR of quadrupolar nuclei by frequency-swept fast amplitude-modulated pulses, *Chem. Phys. Lett.* 383 (2004) 403–410.
- [43] T. Bräuniger, P.K. Madhu, A. Pampel, D. Reichert, Application of fast amplitude-modulated pulse trains for signal enhancement in static and magic-angle-spinning $^{47,49}\text{Ti}$ -NMR spectra, *Solid State Nucl. Magn. Reson.* 26 (2004) 114–120.
- [44] T. Bräuniger, G. Hempel, P.K. Madhu, Fast amplitude-modulated pulse trains with frequency sweep (SW-FAM) in static NMR of half-integer spin quadrupolar nuclei, *J. Magn. Reson.* 181 (2006) 68–78.
- [45] M.S. Silver, R.I. Joseph, D.I. Hoult, Selective spin inversion in nuclear magnetic resonance and coherent spin optics through an exact solution of the Bloch-Riccati equation, *Phys. Rev. A* 31 (1985) 2753–2755.
- [46] K.J. Pike, R.P. Malde, S.E. Ashbrook, J. McManus, S. Wimperis, Multiple-quantum MAS NMR of quadrupolar nuclei. Do five-, seven- and nine-quantum experiments yield higher resolution than the three-quantum experiment?, *Solid State Nucl. Magn. Res.* 16 (2000) 203–215.
- [47] M. Bak, J.T. Rasmussen, N.C. Nielsen, SIMPSON: a general simulation program for solid-state NMR spectroscopy, *J. Magn. Reson.* 147 (2000) 296–330.
- [48] D. Padro, V. Jennings, M.E. Smith, R. Hoppe, P.A. Thomas, R. Dupree, Variations of titanium interactions in solid-state NMR—correlations to local structure, *J. Phys. Chem. B* 106 (2002) 13176–13185.
- [49] A.P.M. Kentgens, E.R.H. van Eck, T.G. Ajithkumar, T. Anupold, J. Past, A. Reinhold, A. Samoson, New opportunities for double rotation NMR of half-integer quadrupolar nuclei, *J. Magn. Reson.* 178 (2006) 212–219.
- [50] M. Goswami, P.K. Madhu, Sensitivity enhancement of the central-transition signal of half-integer spin quadrupolar nuclei in solid-state NMR: features of multiple fast amplitude-modulated pulse transfer, *J. Magn. Reson.* 192 (2008) 230–234.
- [51] G. Wu, D. Rovnyak, R.G. Griffin, Quantitative multiple-quantum magic-angle-spinning NMR spectroscopy of quadrupolar nuclei in solids, *J. Am. Chem. Soc.* 118 (1996) 9326–9332.
- [52] R. Siegel, T.T. Nakashima, R.E. Wasylshen, Sensitivity enhancement of NMR spectra of spin 3/2 nuclei using hyperbolic secant pulses, *Chem. Phys. Lett.* 403 (2005) 353–358.
- [53] P.K. Madhu, A. Goldbourt, L. Frydman, S. Vega, Sensitivity enhancement of the MQMAS NMR experiment by fast amplitude modulation of the pulses, *Chem. Phys. Lett.* 307 (1999) 41–47.
- [54] A. Goldbourt, P.K. Madhu, S. Vega, Enhanced conversion of triple to single-quantum coherence in the triple-quantum MAS NMR spectroscopy of spin-5/2 nuclei, *Chem. Phys. Lett.* 320 (2000) 448–456.
- [55] Z. Gan, H.-T. Kwak, Enhancing MQMAS sensitivity using signals from multiple coherence transfer pathways, *J. Magn. Reson.* 168 (2004) 346–351.
- [56] J.P. Amoureux, L. Delevoye, S. Steuernagel, Z. Gan, S. Ganapathy, L. Montagne, Increasing sensitivity of 2D high-resolution NMR methods applied to quadrupolar nuclei, *J. Magn. Reson.* 172 (2005) 268–278.
- [57] T.J. Ball, S. Wimperis, Use of SPAM and FAM pulses in high-resolution MAS NMR spectroscopy of quadrupolar nuclei, *J. Magn. Reson.* 187 (2007) 343–351.
- [58] A. Goldbourt, P.K. Madhu, S. Kababya, S. Vega, The influence of the lineshapes and intensities of the triple-quantum MAS NMR spectra of $I = 3/2$ nuclei, *Solid State Nucl. Magn. Reson.* 18 (2000) 1–16.
- [59] H.-T. Kwak, S. Prasad, Z. Yao, P.J. Grandinetti, J.R. Sachleben, L. Emsley, Enhanced sensitivity in RIACT/MQ-MAS experiments using rotor assisted population transfer, *J. Magn. Reson.* 150 (2001) 71–80.
- [60] K.H. Lim, T. Charpentier, A. Pines, Efficient triple-quantum excitation in modified RIACT MQMAS NMR for $I = 3/2$ nuclei, *J. Magn. Reson.* 154 (2002) 196–204.
- [61] P.K. Madhu, M.H. Levitt, Signal enhancement in the triple-quantum magic-angle spinning NMR of spins-3/2 in solids: the FAM-RIACT-FAM sequence, *J. Magn. Reson.* 155 (2002) 150–155.
- [62] A. Goldbourt, S. Vega, Signal enhancement in 5QMAS spectra of spin-5/2 quadrupolar nuclei, *J. Magn. Reson.* 154 (2002) 280–286.
- [63] T. Bräuniger, K.J. Pike, R.K. Harris, P.K. Madhu, Efficient 5QMAS NMR of spin-5/2 nuclei: use of fast amplitude-modulated radio-frequency pulses and cogwheel phase cycling, *J. Magn. Reson.* 163 (2003) 64–72.
- [64] A.D. Bain, Coherence levels and coherence pathways in NMR. A simple way to design phase cycling procedures, *J. Magn. Reson.* 56 (1984) 418–427.
- [65] G. Bodenhausen, H. Kogler, R.R. Ernst, Selection of coherence-transfer pathways in NMR pulse experiments, *J. Magn. Reson.* 58 (1984) 370–388.
- [66] J. Kanellopoulos, D. Freude, A. Kentgens, A practical comparison of MQMAS techniques, *Solid State Nucl. Magn. Reson.* 32 (2008) 99–108.
- [67] S.P. Brown, S.J. Heyes, S. Wimperis, Two-dimensional MAS multiple-quantum NMR of quadrupolar nuclei. Removal of inhomogeneous second-order broadening, *J. Magn. Reson.* 119 A (1996) 280–284.
- [68] J.P. Amoureux, C. Fernandez, S. Steuernagel, Z filtering in MQMAS NMR, *J. Magn. Reson. A* 123 (1996) 116–118.
- [69] S.P. Brown, S. Wimperis, Two-dimensional multiple-quantum MAS NMR of quadrupolar nuclei. Acquisition of the whole echo, *J. Magn. Reson.* 124 (1997) 279–285.
- [70] M.H. Levitt, P.K. Madhu, C.E. Hughes, Cogwheel phase cycling, *J. Magn. Reson.* 155 (2002) 300–306.